DOI: 10.1002/asia.201301228

# High-Performance Dye-Sensitized Solar Cells Based on Phenothiazine Dyes Containing Double Anchors and Thiophene Spacers

**Wei-I Hung, You-Ya Liao, Chih-Yu Hsu, Hsien-Hsin Chou, Ting-Hui Lee, Wei-Siang Kao, and Jiann T. Lin*[a]**

**Abstract:** A series of new push–pull phenothiazine-based dyes (**HL1–HL4**) featuring various π spacers (thiophene, 3-hexylthiophene, 4-hexyl-2,2′-bithiophene) and double acceptors/anchors have been synthesized, characterized, and used as sensitizers for dye-sensitized solar cells (DSSCs). Among them, the best conversion efficiency (7.31 %) reaches approximately 99 % of the N719-based (7.38 %) DSSCs fabricated and measured under similar conditions. The dyes with two anchors have more efficient interfacial charge generation and transport compared with their congeners with only single anchor. Incorporation of hexyl chains into the π-conjugated spacer of these double-anchoring dyes can efficiently suppress dye aggregation and reduce charge recombination.

**Keywords:** electrochemistry · dyes/pigments · dye-sensitized solar cells · sensitizers · titanium

## Introduction

Dye-sensitized solar cells (DSSCs) have attracted considerable interest in both academic and industrial communities for the past two decades after seminal work by O'Regan and Grätzel in 1991,[1] mainly owing to their easy fabrication, high efficiency, and low cost. To further improve the performance of DSSCs in fulfilling future energy demands, dye molecules play a pivotal role in increasing energy conversion.[2] DSSCs with a record high efficiency of 12.3 % have been achieved recently by employing a combination of a zinc porphyrin dye (YD2-*o*-C8) and an organic dye (Y123); this demonstrates that there is still room for increasing conversion efficiency by developing new dyes and new fabrication technology.[3] Among sensitizers, metal-free organic dyes (with a prototype donor–π–acceptor (D-π-A) dipolar architecture) possess several advantages, such as high molar extinction coefficients, potentially low costs, environmentally friendliness, as well as easier preparation and purification[2,4] Consequently, metal-free organic dyes have also been intensively investigated and high-performance DSSCs have also been demonstrated.[2d,5] Factors controlling power-conversion efficiency, such as light harvesting, electron injection, dye regeneration, charge recombination, and stability, are all strongly correlated with the structure of the dye. Among them, dye aggregation and charge recombination with the oxidized electrolyte (dark current) are the main problems for molecular design.[4b,5c,6] Several approaches were developed to tackle these problems: 1) Addition of antiaggregation agents or coadsorbents (such as chenodeoxycholic acid (CDCA) or deoxycholic acid (DCA)) to suppress dye aggregation on $TiO_2$.[5d,7] 2) Incorporation of alkyl chains or bulky groups at the donor moiety or the π bridge to block the electrolyte from close contact with the $TiO_2$ surface. The alkyl chains or bulky groups may also help to suppress molecular aggregation.[4a,5c,8] 3) Dyes with two pinched D-π-A motifs or with di- or multianchor groups, $D(-\pi-A)_n$ ($n \geq 2$), to suppress intermolecular excited-state quenching.[4b,9] Organic sensitizers with di- or multianchor groups also provide more efficient electron extraction paths than those with a single anchor, therefore, the photocurrent can be increased.[4b,9a,10] Previously, we found that dyes with two anchors were more efficient than congeners with a single anchor in hole injection and dark-current suppression for p-type DSSCs.[11] We therefore applied the same strategy to the dye for n-type DSSCs. We herein report new phenothiazine-based sensitizers with double anchors.

## Results and Discussion

### Design and Synthesis

The structures of the new phenothiazine-based dyes are shown in Figure 1. The synthetic routes to these compounds extensively utilize palladium-catalyzed Stille coupling or Suzuki coupling, as depicted in Scheme 1. The key intermediates, 3-bromo-10-(2-ethylhexyl)-10*H*-phenothiazine (**2**) and 3,7-dibromo-10-(2-ethylhexyl)-10*H*-phenothiazine (**4**), were prepared from 10-(2-ethylhexyl)-10*H*-phenothiazine with NBS, similar to published procedures.[12] Compounds **3**, **5**, **6**, and **8** were obtained by different approaches. Stille

---

[a] Dr. W.-I Hung, Y.-Y. Liao, Dr. C.-Y. Hsu, Dr. H.-H. Chou, T.-H. Lee, W.-S. Kao, Prof. Dr. J. T. Lin
Institute of Chemistry, Academia Sinica
Taipei, 115 (Taiwan)
E-mail: jtlin@gate.sinica.edu.tw

Supporting information for this article is available on the WWW under http://dx.doi.org/10.1002/asia.201301228.

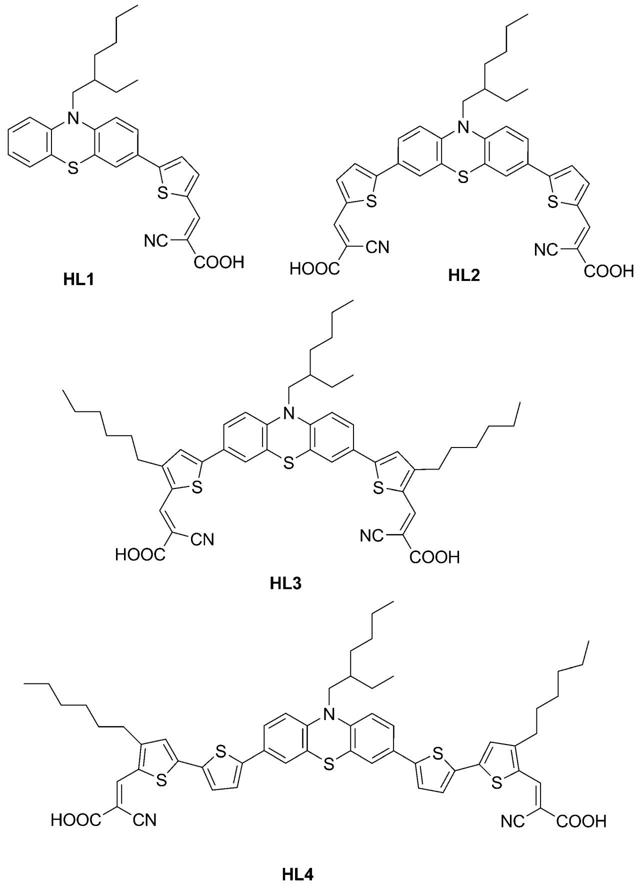

Figure 1. Structures of the organic dyes described herein.

C–C coupling of **2** and **4** with aldehyde-containing stannyl reagents provided formyl compounds **3** and **5** in 41 and 85 %, respectively. Suzuki C–C coupling of compound **4** with appropriate thiophene dioxaborolanes gave the intermediates **6** (96 %) and **8** (67 %). Second Suzuki coupling reactions of **8** with 3-hexylthiophene dioxaborolanes provided **9**. Subsequent Vilsmeier–Haack reactions of **6** and **9** yielded compounds **7** and **10**, respectively. Finally, Knoevenagel condensation of **3**, **5**, **7**, and **10** with cyanoacetic acid afforded the desired dyes **HL1**–**HL4**. The new organic dyes were characterized by NMR spectroscopy and mass spectrometry. While this research was in progress, compounds with structures similar to those of **HL1** and **HL2** were reported.[10e]

**Abstract in Chinese:**

本文章合成一系列以硫二苯胺為電子予體並經由不同結構的共軛架橋連接兩個電子受體形成雙芽型光敏劑，並用於染料敏化太陽能電池。此系列染料中，最好的光電轉換效率高達 7.31%，為 N719 建構標準元件(7.38%)的 99%。透過研究發現，雙芽型光敏劑比單芽型光敏劑擁有更有效的電子注入路徑。雙芽型光敏劑在共軛架橋中引入己烷鏈更可有效減少染料間的堆疊並抑制暗電流。

## UV/Vis Absorption Properties

Figure 2 shows the UV/Vis absorption spectra of the organic dyes in THF, and the corresponding data are summarized in Table 1. Two distinct bands were observed for these compounds. Based on theoretical computations (see below), the band located at a shorter wavelength (band I) is attributed to an aromatic π–π* transition, and the band at a longer wavelength (band II) is assigned to an intramolecular donor→acceptor charge-transfer (ICT) transition with the character of a π–π* transition. Intermixing with π–π* character significantly enhances the intensity of the ICT band in **HL2**–**HL4** compared with **HL1** because the former has longer π–π conjugation. This observation is consistent with the congeners of **HL2** and **HL3**, in which the 2-ethylhexyl substituent is replaced with a hexyl chain. Moreover, the ICT band of **HL2**–**HL4** appears at a longer wavelength (**HL2**: $\lambda = 469$ nm, $\varepsilon = 5.02 \times 10^4\,\mathrm{M^{-1}\,cm^{-1}}$; **HL3**: $\lambda = 475$ nm, $\varepsilon = 4.79 \times 10^4\,\mathrm{M^{-1}\,cm^{-1}}$; **HL4**: $\lambda = 484$ nm, $\varepsilon = 7.16 \times 10^4\,\mathrm{M^{-1}\,cm^{-1}}$) than that of HL1 ($\lambda = 444$ nm, $2.19 \times 10^4\,\mathrm{M^{-1}\,cm^{-1}}$). Noticeably, **HL4** possesses a broader absorption range and higher molar extinction coefficient than those of the others owing to it having the longest conjugated spacer. A wider absorption range should be favorable for photocurrent generation in DSSCs because more photons can be harvested.[13] The spectra of the dyes with and without CDCA adsorbed on a nanocrystalline $TiO_2$ film are shown in Figure 3. The blueshift of the absorption spectra of dyes (without CDCA) on $TiO_2$ compared with those in solution can be ascribed to deprotonation of carboxylic acid and/or the formation of H aggregates on the $TiO_2$ surface.[13,14] Notably, these dyes exhibit different degrees of

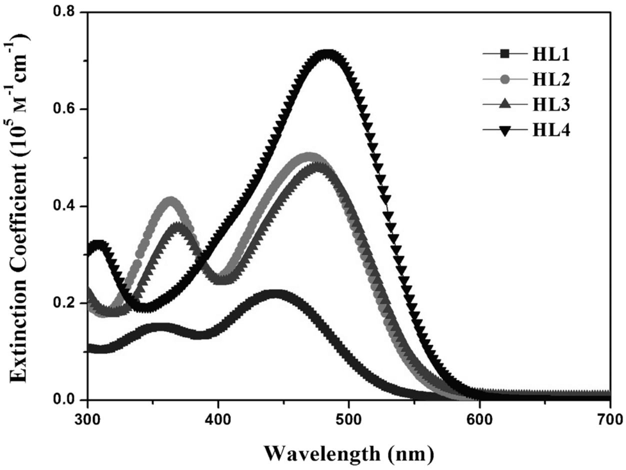

Figure 2. Absorption spectra of the dyes in THF.

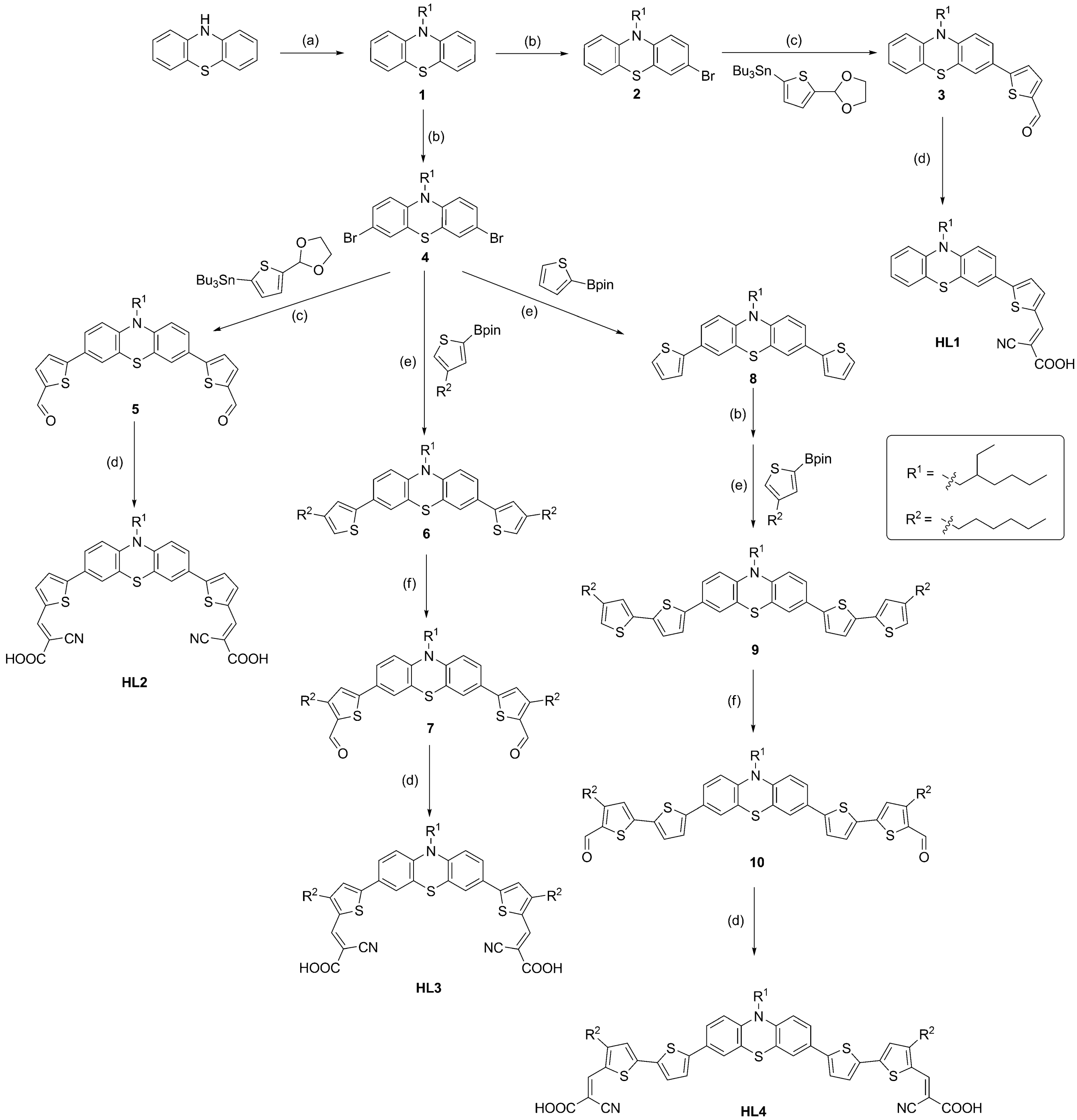

Scheme 1. Synthetic routes for the preparation of dyes **HL1**–**HL4**. a) Tetrahydrofuran (THF), *t*BuOK, 2-ethylhexyl bromide, 65 °C, overnight; b) *N*,*N*-dimethylformamide (DMF), *N*-bromosuccinimide (NBS), 25 °C, overnight; c) DMF, $PPh_3$, $[PdCl_2(PPh_3)_2]$, 80 °C, overnight; then: dichloromethane, 4 N HCl, 25 °C, overnight; d) acetonitrile/THF, cyanoacetic acid, piperidine, 80 °C, overnight; e) toluene, $Na_2CO_3$, $[Pd(PPh_3)_4]$, 80 °C, overnight; f) DMF, $POCl_3$, 65 °C, 3 h; then: $CH_3COONa_{(aq)}$, 0 °C, 30 min.

molecular aggregation on the $TiO_2$ surface. The absorption profiles of **HL3** and **HL4** remain the same, except for a decrease in intensity upon the addition of CDCA, which indicates that there is negligible dye aggregation for the two compounds. In contrast, a prominent redshift of the absorption spectra for **HL1** and **HL2** upon the addition of CDCA suggests the existence of dye aggregation for these two dyes.

### Electrochemical Properties

The electrochemical properties of the organic dyes were measured by cyclic voltammetry (CV) in THF (Figure S5 in the Supporting Information), and the results are listed in Table 1. The oxidation potentials ($E_{ox}$) correspond to the HOMO; the LUMO was obtained from the value of $E_{ox}$ and

Table 1. Electro-optical parameters of the dyes.

| Dye | $\lambda_{abs}$ ($\varepsilon$ [$\mathrm{M}^{-4}\,\mathrm{cm}^{-1}$]) [nm][a] | $\lambda_{em}$ [nm][a] | $\lambda_{TiO2}$ [nm] | $E_{0-0}$ [eV][b] | $E_{ox}$ [V vs. NHE][c] | $E_{0-0}$* [V vs. NHE][d] | HOMO/LUMO [eV] |
|---|---|---|---|---|---|---|---|
| **HL1** | 356 (1.51),<br>444 (2.19) | 656 | 426 | 2.34 | 1.09 | −1.25 | 5.49/3.15 |
| **HL2** | 364 (4.11),<br>469 (5.02) | 655 | 437 | 2.21 | 1.11 | −1.10 | 5.51/3.30 |
| **HL3** | 369 (3.56),<br>475 (4.79) | 648 | 460 | 2.19 | 1.10 | −1.09 | 5.50/3.31 |
| **HL4** | 308 (3.23),<br>484 (7.16) | 743 | 422 | 2.15 | 1.01 | −1.14 | 5.41/3.26 |

[a] Recorded in THF at 298 K. [b] The band gap, $E_{0-0}$, was derived from peak separation of the cathodic and anodic waves. Scan rate: 100 mV s$^{-1}$. [c] Recorded in THF. $E_{ox} = 1/2(E_{pa} + E_{pc})$, $\Delta E_p = E_{pa} - E_{pc}$, in which $E_{pa}$ and $E_{pc}$ are the peak anodic and cathodic potentials, respectively. The oxidation potential reported was adjusted to the potential of ferrocene, which was used as an internal reference. [d] $E_{0-0}$*: The excited state oxidation potential versus a normal hydrogen electrode (NHE).

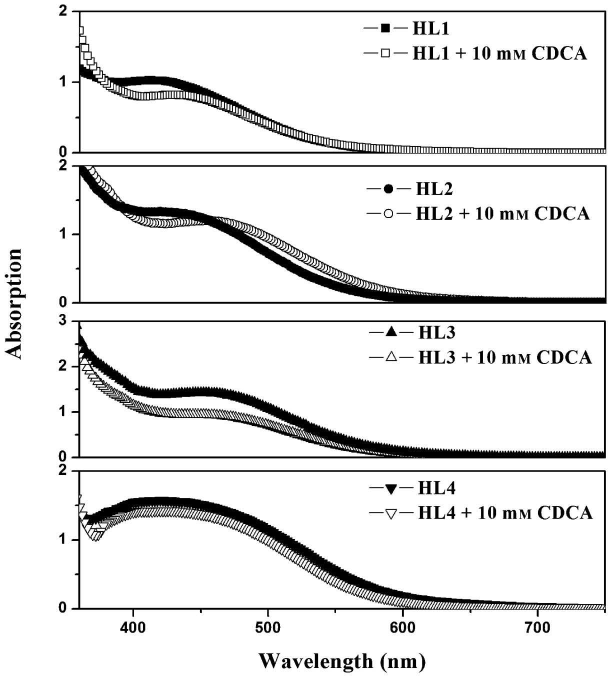

Figure 3. Absorption spectra of the dyes on $TiO_2$ films.

the zero–zero band gap ($E_{0-0}$) estimated from the intersection of the absorption and emission spectra of the dye.[15] The first quasi-reversible one-electron oxidation wave detected at about 178–573 mV more positive than ferrocene/ferrocenium was attributed to removal of an electron from phenothiazine. Inserting two electron-rich thiophene units in the π bridge between the phenothiazine moiety and each anchoring group (**HL4**) significantly raised the HOMO level and resulted in a decreased oxidation potential.[16] Dyes **HL1**–**HL3** have comparable oxidation potentials that are higher than that of **HL4**. Because of more localized nature of the LUMO (see the Theoretical Approach section below), dye HL1 has a larger HOMO/LUMO energy gap. A suitable HOMO level is necessary to match the redox potential (+0.4 V vs. NHE) of the iodide/triiodide electrolyte. Owing to a sufficiently low HOMO energy level of the dye, there is enough driving force for dye regeneration, which decreases charge recombination between the oxidized dye molecules and photoinjected electrons in the $TiO_2$ conduction band.[5c] The excited-state potential ($E_{0-0}$*) of the dye, deduced by subtracting $E_{0-0}$ from $E_{ox}$, is more negative than the conduction band edge of $TiO_2$ (−0.5 V vs. NHE); this should be sufficient for electron injection from the excited dye molecule into the conduction band of $TiO_2$.

## Device Performance

The DSSCs were fabricated by using these organic dyes as the sensitizers and nanocrystalline anatase $TiO_2$ as the photoanode. The basic device performance parameters, such as open-circuit photovoltage ($V_{oc}$), short-circuit current ($J_{sc}$), fill factor (FF), and power conversion efficiency ($\eta$), were measured under simulated AM 1.5 illumination, and are collected in Table 2. Figures 4 and 5 show the photocurrent–voltage ($J$–$V$) plots and photon-to-current conversion efficiencies (IPCE), respectively, of the HL-sensitized solar cells. A very high efficiency of 7.31 % ($V_{oc} = 0.69$ V, $J_{sc} = 15.88$ mA cm$^{-2}$, FF = 0.67) was achieved with the **HL4** sensitizer; these values are comparable with that (7.38 %) of an N719-based standard cell fabricated and measured under similar conditions. DSSCs based on **HL1**–**HL3** exhibited $\eta$ values of 4.91, 5.53, and 6.85 %, respectively. Dye **HL1**, with a single anchoring group, has the lowest cell conversion effi-

Table 2. Photovoltaic parameters for DSSCs of the dyes.

| Dye | $V_{oc}$ [V] | $J_{sc}$ [mA cm$^{-2}$] | FF | $\eta$ [%] | Dye loading [mol cm$^{-2}$] | $\tau_r$ [ms][a] | $R_{ct2}$ |
|---|---|---|---|---|---|---|---|
| **HL1** | 0.69 | 10.23 | 0.70 | 4.91 | $4.79 \times 10^{-7}$ | 29.41 | 29.05 |
| **HL1**+CDCA[b] | 0.72 | 11.07 | 0.70 | 5.55 | | | |
| **HL2** | 0.66 | 12.27 | 0.68 | 5.53 | $1.13 \times 10^{-6}$ | 15.92 | 27.46 |
| **HL2**+CDCA[b] | 0.67 | 13.52 | 0.69 | 6.29 | | | |
| **HL3** | 0.68 | 14.82 | 0.68 | 6.85 | $5.52 \times 10^{-7}$ | 25.22 | 24.92 |
| **HL3**+CDCA[b] | 0.70 | 13.23 | 0.70 | 6.48 | | | |
| **HL4** | 0.69 | 15.88 | 0.67 | 7.31 | $7.45 \times 10^{-7}$ | 39.98 | 19.73 |
| **HL4**+CDCA[b] | 0.68 | 14.91 | 0.66 | 6.67 | | | |
| N719 | 0.77 | 14.33 | 0.67 | 7.38 | | 54.35 | 26.92 |

[a] The lifetime of injected electrons, measured by intensity-modulated photovoltage spectroscopy (IMVS) under a light intensity of 300 W m$^{-2}$, was inserted into the expression $\tau_r = 1/(2\pi f)$, in which $f$ is the frequency. [b] Uptake achieved in the presence of 10 mM CDCA.

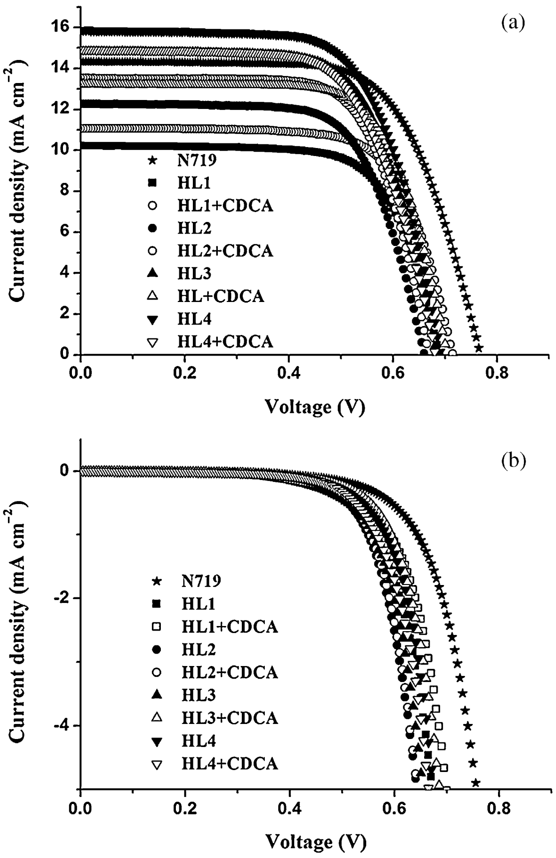

Figure 4. *J–V* curves of the DSSC devices made with the dyes measured a) under AM 1.5 solar simulator of 100 mW cm$^{-2}$ and b) in the dark.

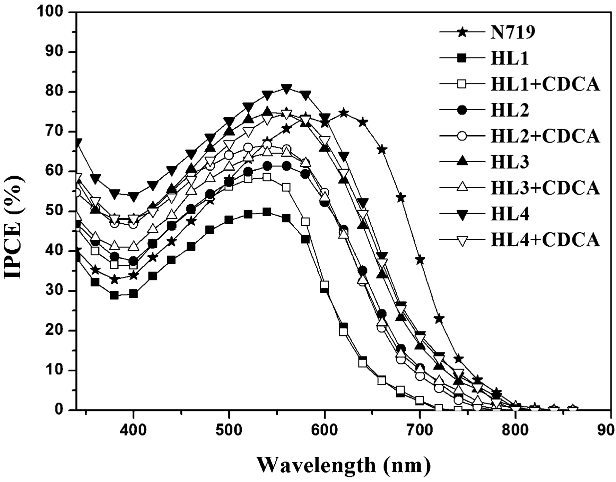

Figure 5. IPCE curves of the DSSCs.

ciency among all of those tested because of its narrow spectral response range and lower absorptivity (Figure 5). Another cause of the low efficiency for **HL1** stems from dye aggregation (see above), which quenches the excited state and deteriorates electron injection. This is also evidenced by the improved open-circuit voltage ($V_{oc}=0.72$ V) and short-circuit current ($J_{sc}=11.07$ mA cm$^{-2}$) after the addition of 10 mM of coadsorbent, CDCA. Because dye aggregation was also observed in **HL2** (see above), the cell performance was significantly improved ($\eta=6.29$ %, $V_{oc}=0.67$ V, $J_{sc}=13.52$ mA cm$^{-2}$, FF$=0.69$) after the addition of 10 mM of coadsorbent.

In contrast to **HL2**, the hexyl chains incorporated into the thiophene of **HL3** help to suppress dye aggregation and there is no advantage gained by the addition of coadsorbent. The values of both $J_{sc}$ and $\eta$ drop upon the addition of CDCA, because the CDCA molecules compete with the dye molecules for the adsorption sites[6b, 9a, 17] and lead to a lower dye density. The slightly higher $V_{oc}$ value may be due to more effective suppression of the dark current. Dye aggregation was also negligible in **HL4** because the coadsorption of CDCA resulted in a decrease in the values of $J_{sc}$ and $\eta$. Consequently, the addition of CDCA to the **HL4**-based DSSC jeopardizes the cell performance, similar to the case of **HL3**. The best performance achieved for the **HL4**-based DSSC device can be attributed to several reasons: 1) **HL4** has the broadest photoresponse and highest molar extinction coefficient; 2) **HL4** has the most efficient interfacial charge generation and transport upon photoexcitation (see below for a description of electrochemical impedance spectroscopy (EIS) under illumination); 3) **HL4** can more effectively suppress the dark current (see below for a description of EIS in the dark); 4) **HL4** has less dye aggregation (see above); and 5) **HL4** has the most upward shift of the conduction band edge of $TiO_2$ (see below).

EIS was also measured in the dark and under illumination conditions to elucidate information on electron injection and recombination at the $TiO_2$/dye/electrolyte interface. The Nyquist plots obtained in the dark and under a forward bias of 0.55 V are shown in Figure 6a, and the second semicircle for each dye is related to the resistance of recombination ($R_{rec}$) between the electrons on the $TiO_2$ surface and the oxidized electrolyte. The larger value of $R_{rec}$ indicates slower recombination kinetics. Therefore, the recombination rate decreases in the order of **HL2** > **HL3** > **HL1** > **HL4**. Incorporation of hexyl chains into the thiophene rings linked to the anchoring group (**HL3** and **HL4**) seems to be beneficial for dark-current suppression.[6a] Elongation of the hydrophobic π bridge (**HL4**) also helps to reduce charge recombination.[18] It is known that the proton released from the carboxylic acid upon dye adsorption will induce a dark current.[19] Therefore, the lower dark current of **HL1** relative to **HL2** and **HL3** may be rationalized by fewer protons being released upon dye adsorption. The conduction band electron lifetime ($\tau_r$) was also measured by IMVS, as shown in Table 2 and Figure 7. At the same light intensity (300 W m$^{-2}$), the electron lifetime decreases in the order of **HL4** (39.98 ms) > **HL1** (29.41 ms) > **HL3** (25.22 ms) > **HL2** (15.92 ms), which is consistent with the EIS data (see above). We further performed charge-extraction measurements to probe the possible variations in $V_{oc}$ with a shift in the Fermi level.[20] Compared with **HL1**, **HL2** and **HL3** exhibit a downward shift of the conduction band edge of $TiO_2$ by about 33 and 7 meV, respectively. In contrast, the con-

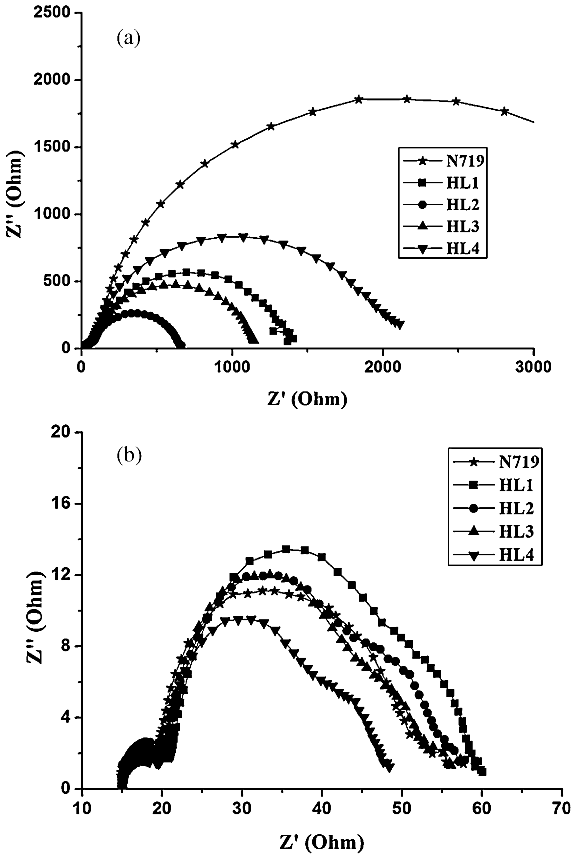

Figure 6. Electrochemical impedance spectra (Nyquist plots) of the DSSC devices made with the dyes measured a) in the dark under −0.55 V bias and b) under illumination at $V_{oc}$.

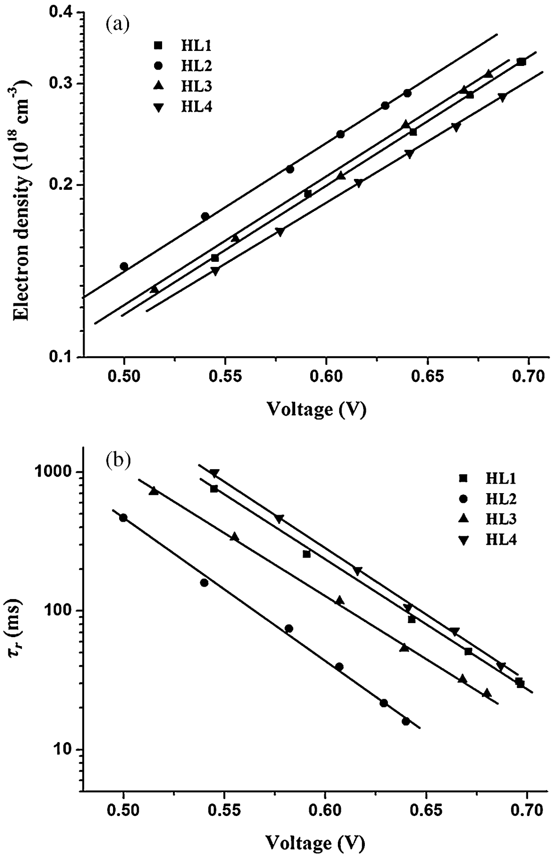

Figure 7. a) Electron lifetime and b) extracted electron density versus photovoltage.

duction band edge of $TiO_2$ exhibits an upward shift by about 16 meV for **HL4** (Figure 7). Two protons released upon the adsorption of dyes with two anchors on $TiO_2$ may result in a downward shift of the $TiO_2$ conduction band.[21] Therefore, in addition to the released protons, the variation in the conduction band edge of $TiO_2$ is also affected by the variation in surface dipole induced by different **HL** dyes.

Upon illumination of the cell under open-circuit voltage conditions (Figure 6b), the intermediate frequency semicircle in the Nyquist plot reflects charge-transfer resistance ($R_{ct2}$) at the semiconductor–dye electrode (Table 2), and the smaller value of $R_{ct2}$ represents lower electron-transport resistance. The value of $R_{ct2}$ decreases in the order of **HL1** > **HL2** > **HL3** > **HL4**; this suggests that dyes with two anchoring groups have more efficient interfacial charge generation and transport than the congener with only one anchoring group.

## Theoretical Approach

To correlate the molecular structures of the dyes with the performance of the DSSCs, we carried out DFT and (TD) DFT calculations at the B3LYP/6-31G* level by using Q-Chem 4.0 software. The results for the time-dependent approach are summarized in Table S1 in the Supporting Information. The ground-state intramolecular dihedral angles, as shown in Figure S5 in the Supporting Information, between the phenothiazine and the neighboring thiophene-containing segments range from 20.3 to 28.6°, which allows efficient charge transfer from phenothiazine to the acceptor. Selected frontier orbitals of the dyes are shown in Figure 8 and Figure S8 in the Supporting Information. The HOMO in these compounds is mainly distributed from phenothiazine to the conjugated spacer, whereas the LUMO and LUMO+1 are largely distributed from 2-cyanoacrylic acid to the spacer. The lowest energy transition (S0→S1) is about 100 % of the HOMO→LUMO transition for all compounds, whereas the S0→S2 transitions of **HL2**–**HL4** mainly stem from the HOMO→LUMO+1 transition. This fact confirms the charge-transfer character of the lowest energy absorption band. From another viewpoint, implementation of a second acceptor/anchor moiety provides an additional excitation probability, which will benefit charge injection of the dye molecules. Despite the charge-transfer transition (S0→S1 in all cases) and more localized π–π transitions (S0→S2 in HL2 and S0→S3 in **HL2**–**HL4**), the bis-anchoring dyes exhibit another charge-transfer transition (S0→S2 in **HL2**–**HL4**) with only slightly higher energies. The latter also explains broadening of the absorption spectra of **HL2**–**HL4** (see above). Also from the TD-DFT results, the differences

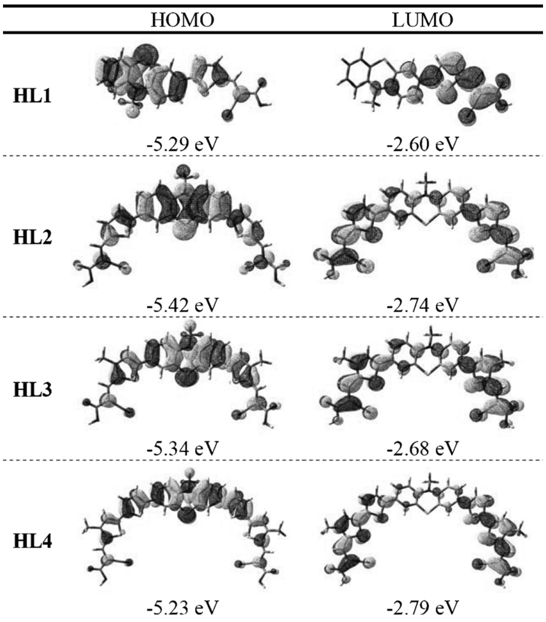

Figure 8. Frontier molecular orbitals of the dyes.

in the Mulliken charges in the excited and ground states were calculated and grouped into several segments, phenothiazine (Ptz1), thiophene (T1, T), and acceptor (Ac; Figure S7 in the Supporting Information). Significant negative charges exist at both acceptors in the dyes with two anchoring groups for both S0→S1 and S0→S2 transitions; this indicates that both acceptors can function as the electron injection channels.

## Conclusion

We have synthesized new phenothiazine-based organic dyes with two anchoring 2-cyanoacrylic acids. These dyes exhibited broader spectral response ranges and higher absorptivity than those of their congeners, which contained a single anchoring group. The new dyes could be used as the sensitizers for high-performance DSSCs. The best cell efficiency (7.31 %) was almost comparable to that of an N719-based standard cell (7.38 %). Sensitizers with two anchoring groups were beneficial for interfacial charge generation and transport. Suppression of the dark current could also be achieved with the incorporation of long hydrocarbon chains in the conjugated spacer.

## Experimental Section

### *Materials and Reagents*

Unless otherwise specified, all reactions and manipulations were carried out under a nitrogen atmosphere. Solvents were dried by standard procedures. The dye bis(tetrabutylammonium)-*cis*-di(thiocyanato)-*N*,*N*′-bis(4-carboxylato-4′-carboxylic acid-2,2′-bipyridine)ruthenium (coded as N719) and $TiO_2$ paste were purchased from Solaronix S. A., Switzerland.

### *Characterization*

$^1H$ and $^{13}C$ NMR spectra were recorded on a Bruker 400 MHz spectrometer. Mass spectra (FAB) were recorded on a VG70-250S mass spectrometer. Elementary analyses were performed on a Perkin–Elmer 2400 CHN analyzer. Absorption spectra were recorded on a Dynamica DB-20 probe UV/Vis spectrophotometer. Fluorescence spectra were recorded on a Hitachi F-4500 spectrophotometer. CV experiments were performed with a CHI-621A electrochemical analyzer. All measurements were carried out at room temperature with a conventional three electrode configuration that consisted of a platinum working electrode, an auxiliary electrode, and a nonaqueous $Ag/AgNO_3$ reference electrode. Photoelectrochemical characterizations on the solar cells were performed by using an Oriel Class AAA solar simulator (Oriel 94043A, Newport Corp.). Photocurrent–voltage characteristics of the DSSCs were recorded with a potentiostat/galvanostat (CHI650B, CH Instruments, Inc.) at a light intensity of $100\ mW\,cm^{-2}$ calibrated by an Oriel reference solar cell (Oriel 91150, Newport Corp.). The monochromatic quantum efficiency was recorded through a monochromator (Oriel 74100, Newport Corp.) under short-circuit condition. The intensity of each wavelength was in the range of 1 to $3\ mW\,cm^{-2}$. Electrochemical impedance spectra were recorded for DSSCs under illumination at an open-circuit voltage ($V_{oc}$) or in the dark at −0.55 V at room temperature. The frequencies explored ranged from 10 mHz to 100 kHz. IMVS was carried out on the electrochemical workstation (Zahner, Zennium) with a frequency response analyzer under an intensity modulated (10 to $300\ W\,m^{-2}$) white-light-emitting diode driven by a Zahner (0982wlr02) source supply. The frequency range was set from 100 kHz to 10 MHz.

### *Assembly and Characterization of DSSCs*

The photoanode used was a $TiO_2$ thin film (12 μm of 20 nm particles as the absorbing layer and 6 μm of 400 nm particles as the scattering layer) coated on an FTO glass substrate with dimensions of $0.4\times0.4\ cm^2$, and a film thickness measured by means of a profilometer (Dektak3, Veeco/Sloan Instruments Inc., USA). The $TiO_2$ thin film was dipped into the solution containing $3\times10^{-4}$ M dye sensitizers in THF for at least 12 h. For the coadsorbed solar cell, CDCA was added to the dye solutions at a concentration of 10 mM. After rinsing with THF, the photoanode was adhered with polyimide tape 30 μm thick and a square aperture of $0.36\ cm^2$ was placed on top of the counter electrode; these were tightly clipped together to form a cell. Electrolyte was then injected into the seam between the two electrodes. The electrolyte was composed of 0.5 M lithium iodide (LiI), 0.05 M iodine ($I_2$), and 0.5 M 4-*tert*-butylpyridine dissolved in acetonitrile.

### *Quantum Chemistry Computation*

Computations were performed with Q-Chem 4.0 software.[22] Geometry optimization of the molecules was performed by using a hybrid B3LYP functional and the 6-31G* basis set. For each molecule, a number of possible conformations were examined and the one with the lowest energy was used. The same functional was also applied for the calculation of excited states by using TD-DFT. A number of previous works exist that employed TD-DFT to characterize excited states with charge-transfer character.[23] In some cases, underestimation of the excitation energies was seen.[23,24] Therefore, herein we used TD-DFT to visualize the extent of transition moments as well as their charge-transfer characters, and avoided drawing conclusions from the excitation energy.

### *General Synthetic Procedure of Dyes*

All sensitizers were synthesized in high yields by using traditional Stille or Suzuki coupling reactions.

### *10-(2-Ethylhexyl)-10H-phenothiazine (**1**)*

In an oven-dried Schlenk flask (100 mL), 10*H*-phenothiazine (4.0 g, 20.0 mmol) and potassium *tert*-butoxide (2.7 g, 24.0 mmol) were dissolved in dry THF (20 mL). After the mixture was stirred for 1 h, 2-ethylhexyl bromide (3.6 mL, 20.0 mmol) was added by means of a syringe. The color of the reaction mixture changed from brown to yellow, and the solution was stirred at 66 °C for 12 h. The solution was cooled to room temperature and the solvent was removed under reduced pressure. The mixture was poured into diethyl ether and the product was washed with water. The organic extract was dried over anhydrous $MgSO_4$ and pumped dry to yield a violet viscous oil, which was purified by column chromatography on silica gel with hexane as the eluent to give **1** as a light-yellow oil (5.6 g, 90%). $^1$H NMR (400 MHz, $CDCl_3$): $\delta = 7.12$ (t, 4H, $J = 6.6$ Hz), 6.90 (d, 2H, $J = 8.0$ Hz), 6.85 (d, 2H, $J = 8.0$ Hz), 3.81(d, 2H, $J = 7.2$ Hz), 1.94–1.88 (m, 1H), 1.45–1.21 (m, 8H), 0.86–0.82 ppm (m, 6H).

*3-Bromo-10-(2-ethylhexyl)-10H-phenothiazine (**2**)*

NBS (1.28 g, 7.22 mmol) in DMF was slowly added by means of a syringe to a solution of **1** (2.25 g, 7.22 mmol) in DMF (180 mL). After the mixture was stirred at room temperature for 12 h, the reaction was terminated by the addition of water. The reaction mixture was extracted with diethyl ether and an aqueous solution of $NH_4Cl$. The organic extract was dried over anhydrous $MgSO_4$ and pumped dry to yield a dark-red viscous oil, which was purified by column chromatography on silica gel with hexane as the eluent to give **2** as a light-yellow oil (2.2 g, 78%). $^1$H NMR (400 MHz, [D$_6$]acetone): $\delta = 7.36$ (dd, $J = 9.6$, 2.4 Hz, 1H), 7.31 (dd, $J =$ 8.4, 2.4 Hz, 1H), 7.22 (t, $J = 7.4$ Hz, 1H), 7.17 (dd, $J = 7.6$, 1.4 Hz, 1H), 7.07 (d, $J = 8.0$ Hz, 1H), 7.02–6.95 (m, 2H), 3.85–3.82 (m, 2H), 1.94–1.88 (m, 1H), 1.51–1.24 (m, 8H), 0.89–0.82 ppm (m, 6H).

*5-(10-(2-Ethylhexyl)-10H-phenothiazin-3-yl)thiophene-2-carbaldehyde (**3**)*

A mixture of **2** (1.23 g, 3.15 mmol), [$PdCl_2(PPh_3)_2$] (0.070 g, 0.095 mmol), (5-(1,3-dioxolan-2-yl)thiophen-2-yl)tributylstannane (3.50 g, 7.88 mmol) and triphenylphosphine (0.050 g, 0.19 mmol) in DMF (15 mL) was placed in a two-necked flask under nitrogen atmosphere and stirred at 80 °C for overnight. After cooling, the reaction was quenched with aqueous KF and the resulting mixture was extracted with $CH_2Cl_2$. The organic extract was dried over anhydrous $MgSO_4$ and pumped dry to yield an orange viscous oil. It was purified by column chromatography on silica gel using hexane/$CH_2Cl_2$ (2:1 v/v) as the eluent to give **3** as an orange oil (0.55 g, 41%). $^1$H NMR (400 MHz, $CDCl_3$): $\delta = 9.83$ (s, 1H), 7.67 (d, $J = 3.9$ Hz, 1H), 7.44–7.42 (m, 2H), 7.26 (d, $J = 4.0$ Hz, 1H), 7.17–7.13 (m, 2H), 6.95–6.85 (m, 3H), 3.74 (d, $J = 7.1$ Hz, 2H), 1.95–1.89 (m, 1H), 1.48–1.22 (m, 8H), 0.91–0.82 ppm (m, 6H); $^{13}$C NMR (100 MHz, $CDCl_3$): $\delta = 182.8$, 154.0, 147.2, 145.1, 141.8, 137.8, 127.9, 127.6, 126.9, 125.8, 125.4, 125.1, 125.1, 123.3, 123.2, 116.4, 116.3, 51.4, 36.2, 30.9, 28.8, 24.2, 23.3, 14.2, 10.7 ppm; MS (MALDI): $m/z$: 421.1 $[M]^+$.

*3,7-Dibromo-10-(2-ethylhexyl)-10H-phenothiazine (**4**)*

Compound **4** was synthesized in 82% yield according to a similar procedure to that described for **2**. $^1$H NMR (400 MHz, $CDCl_3$): $\delta = 7.23$–7.21 (m, 4H), 6.68 (d, $J = 9.2$ Hz, 2H), 3.62 (d, $J = 7.2$ Hz, 2H), 1.87–1.80 (m, 1H), 1.42–1.21 (m, 8H), 0.94–0.85 ppm (m, 6H).

*5,5′-[10-(2-Ethylhexyl)-10H-phenothiazine-3,7-diyl]bis(thiophene-2-carbaldehyde) (**5**)*

Compound **5** was synthesized in 85% yield by following a similar procedure to that described for **3**. $^1$H NMR (400 MHz, $CDCl_3$): $\delta = 9.85$ (s, 2H), 7.69 (d, $J = 4.0$ Hz, 2H), 7.46 (dd, $J = 8.4$, 1.8 Hz, 2H), 7.43 (d, $J =$ 2.0 Hz, 2H), 7.29 (d, $J = 4.0$ Hz, 2H), 6.90 (d, $J = 8.4$ Hz, 2H), 3.77 (d, $J =$ 7.2 Hz, 2H), 1.96–1.90 (m, 1H), 1.46–1.25 (m, 8H), 0.89–0.83 ppm (m, 6H); $^{13}$C NMR (100 MHz, $CDCl_3$): $\delta = 182.7$, 153.4, 146.1, 142.2, 137.6, 128.3, 126.3, 126.0, 125.4, 123.6, 116.6, 51.5, 36.5, 30.9, 28.8, 24.2, 23.3, 14.2, 10.7 ppm; MS (MALDI): $m/z$: 531.0 $[M]^+$.

*10-(2-Ethylhexyl)-3,7-bis(4-hexylthiophen-2-yl)-10H-phenothiazine (**6**)*

Toluene (20 mL), EtOH (5 mL) and $H_2O$ (10 mL) were added to a flask containing a mixture of **4** (3.0 g, 6.52 mmol), 2-(4-hexylthiophen-2-yl)-1,3-dioxolane (4.80 g, 16.3 mmol), [$Pd(PPh_3)_4$] (0.38 g, 0.32 mmol), and $Na_2CO_3$ (2.10 g, 19.6 mmol), and the solution was heated at reflux for 12 h. The solution was cooled to room temperature and extracted with a mixture of $CH_2Cl_2$ and $H_2O$. The organic extract was dried over anhydrous $MgSO_4$ and pumped dry to yield a dark-yellow viscous oil, which was purified by column chromatography on silica gel with hexane/$CH_2Cl_2$ (9:1 v/v) as the eluent to give **6** as a yellow oil (1.25 g, 30%). $^1$H NMR (400 MHz, [D$_6$]acetone): $\delta = 7.45$ (dd, $J = 8.4$, 2.4 Hz, 2H), 7.42 (d , $J =$ 2.0 Hz, 2H), 7.25 (d, $J = 1.2$ Hz, 2H), 7.05 (d, $J = 8.4$ Hz, 2H), 6.98 (d, $J =$ 0.8 Hz, 2H), 3.92–3.83 (m, 2H), 2.61 (t, $J = 7.6$ Hz, 4H), 2.01–1.91 (m, 1H), 1.65 (quint, $J = 7.7$ Hz, 4H), 1.53–1.22 (m, 20H), 0.91–0.83 ppm (m, 12H); $^{13}$C NMR (100 MHz, [D$_6$]acetone): $\delta = 145.6$, 145.2, 143.2, 130.4, 126.5, 125.6, 124.9, 120.0, 117.4, 51.8, 37.1, 32.5, 31.4, 31.30, 31.27, 29.8, 24.7, 23.5, 23.4, 14.5, 11.0 ppm; MS (MALDI): $m/z$: 643.1 $[M]^+$.

*5,5′-[10-(2-Ethylhexyl)-10H-phenothiazine-3,7-diyl]bis(3-hexylthiophene-2-carbaldehyde) (**7**)*

A solution of **6** (1.25 g, 1.94 mmol) in DMF (5 mL) was cooled to 0 °C under a $N_2$ atmosphere. $POCl_3$ (0.54 mL, 5.82 mmol) was added slowly by means of a syringe. The mixture was stirred for 30 min at 0 °C and 3 h at 65 °C. After cooling, the reaction was quenched with an aqueous solution of $CH_3COONa$ and the resulting mixture was extracted with $CH_2Cl_2$ and $H_2O$. The organic extract was dried over anhydrous $MgSO_4$ and pumped dry to yield an orange viscous oil, which was purified by column chromatography on aluminum oxide gel with hexane/$CH_2Cl_2$ (1:1 v/v) as the eluent to give **7** as an orange oil (1.3 g, 96%). $^1$H NMR (400 MHz, [D$_6$]acetone): $\delta = 10.07$ (s, 2H), 7.63 (dd, $J = 8.4$, 2.0 Hz, 2H), 7.59 (d, $J =$ 2.0 Hz, 2H), 7.50 (s, 2H), 7.17 (d, $J = 8.4$ Hz, 2H), 4.03–3.91 (m, 2H), 3.04 (t, $J = 7.6$ Hz, 4H), 2.01–1.96 (m, 1H), 1.75 (quint, $J = 7.6$ Hz, 4H), 1.51–1.24 (m, 20H), 0.93–0.83 ppm (m, 12H); $^{13}$C NMR (125 MHz, [D$_6$]acetone): $\delta = 182.5$, 155.0, 151.9, 147.0, 137.2, 129.1, 127.4, 126.7, 126.6, 125.7, 117.9, 52.0, 37.2, 32.4, 32.2, 31.4, 29.5, 29.1, 24.7, 23.8, 23.3, 14.4, 11.0 ppm; MS (MALDI): $m/z$: 699.2 $[M]^+$.

*10-(2-Ethylhexyl)-3,7-di(thiophen-2-yl)-10H-phenothiazine (**8**)*

Compound **8** was synthesized in 67% yield according to a similar procedure to that described for **6**. $^1$H NMR (400 MHz, [D$_6$]acetone): $\delta = 7.49$ (dd, $J = 8.4$, 2.0 Hz, 2H), 7.45 (d, $J = 2.0$ Hz, 2H), 7.38 (m, 4H), 7.09 (d, $J = 3.6$ Hz, 2H), 7.07 (d, $J = 3.6$ Hz, 2H), 3.94–3.84 (m, 2H), 2.00–1.94 (m, 1H), 1.55–1.22 (m, 8H), 0.90 (t, $J = 7.5$ Hz, 3H), 0.85 ppm (t, $J = 7.2$ Hz, 3H).

*10-(2-Ethylhexyl)-3,7-bis[4′-hexyl(2,2′-bithiophen)-5-yl]-10H-phenothiazine (**9**)*

Compound **9** was synthesized in 32% yield according to a similar procedure to that described for **6**. $^1$H NMR (400 MHz, [D$_6$]acetone): $\delta = 7.51$ (dd, $J = 8.3$, 2.4 Hz, 2H), 7.49 (d, $J = 2.1$ Hz, 2H), 7.34 (d, $J = 4.0$ Hz, 2H), 7.20 (d, $J = 4.0$ Hz, 2H), 7.17 (d, $J = 1.2$ Hz, 2H), 7.12 (d, $J = 8.4$ Hz, 2H), 7.02 (s, 2H), 3.98–3.88 (m, 2H), 2.62 (t, $J = 7.6$ Hz, 4H), 2.00–1.96 (m, 1H), 1.66 (quint, $J = 7.5$ Hz, 4H), 1.54–1.26 (m, 20H), 0.93–0.84 ppm (m, 12H); $^{13}$C NMR (100 MHz, [D$_6$]acetone): $\delta = 145.8$, 145.2, 142.6, 137.8, 137.3, 129.7, 126.5, 125.9, 125.6, 125.4, 124.9, 124.4, 120.3, 117.6, 55.0, 51.8, 37.1, 32.5, 31.4, 31.24, 31.15, 29.8, 24.7, 23.9, 23.4, 14.5, 14.4, 11.0 ppm; MS (MALDI): $m/z$: 807.1 $[M]^+$.

*5′,5‴-[10-(2-Ethylhexyl)-10H-phenothiazine-3,7-diyl]bis[4-hexyl-(2,2′-bithiophene)-5-carbaldehyde] (**10**)*

Compound **10** was synthesized in 73% yield according to a similar procedure to that described for **7**. $^1$H NMR (400 MHz, [D$_6$]acetone): $\delta = 10.07$ (s, 2H), 7.55 (dd, $J = 8.5$, 2.1 Hz, 2H), 7.51 (d, $J = 2.1$ Hz, 2H), 7.48 (d, $J = 3.8$ Hz, 2H), 7.43 (d, $J = 4.0$ Hz, 2H), 7.35 (s, 2H), 7.15 (d, $J = 8.6$ Hz, 2H), 3.99–3.89 (m, 2H), 3.04 (t, $J = 7.6$ Hz, 4H), 2.02–1.96 (m, 1H), 1.75 (quint, $J = 7.5$ Hz, 4H), 1.54–1.25 (m, 20H), 0.93–0.84 ppm (m, 12H); $^{13}$C NMR (125 MHz, [D$_6$]acetone): $\delta = 182.3$, 154.8, 146.1, 145.9, 145.5, 136.9, 135.5, 129.2, 128.3, 127.5, 126.4, 126.0, 125.1, 124.9, 117.6, 51.8, 37.1, 32.4, 32.2, 31.4, 29.9, 29.1, 24.7, 23.9, 23.4, 14.5, 11.0 ppm; MS (MALDI): $m/z$: 863.2 $[M]^+$.

*(E)-2-Cyano-3-{5-[10-(2-ethylhexyl)-10H-phenothiazin-3-yl]thiophen-2-yl}acrylic acid (**HL1**)*

Acetonitrile (5 mL) was added to a flask containing a mixture of **3** (0.55 g, 1.30 mmol), cyanoacetic acid (556 mg, 3.26 mmol), and piperidine (2 drops), and the solution was heated at 80 °C for 18 h. The solution was cooled to room temperature and filtered. The filtrate was pumped dry and the crude product was further purified by column chromatography on silica gel with ethyl acetate/acetic acid (100:1 v/v) as the eluent to afford **HL1** as a brown powder (71%, 0.923 mmol). $^1$H NMR (400 MHz, [D$_6$]acetone): $\delta = 8.43$ (s, 1H), 7.96 (d, $J = 4.0$ Hz, 1H), 7.65–7.61 (m, 3H), 7.24–7.15 (m, 3H), 7.10 (d, $J = 8.4$ Hz, 1H), 7.00 (t, $J = 7.6$ Hz, 1H), 3.97–3.87 (m, 2H), 2.00–1.94 (m, 1H), 1.54–1.27 (m, 8H), 0.90 (t, $J = 7.4$ Hz, 3H), 0.84 ppm (t, $J = 7.2$ Hz, 3H); $^{13}$C NMR (100 MHz, [D$_6$]acetone): $\delta = 164.1$, 154.1, 148.1, 147.5, 145.9, 141.5, 135.2, 128.6, 128.4, 128.1, 127.4, 126.7, 125.6, 125.5, 124.8, 124.0, 117.6, 117.0, 98.6, 51.8, 37.0, 31.4, 29.3, 24.7, 23.8, 14.3, 10.9 ppm; HRMS (MALDI): *m/z* calcd for $C_{28}H_{28}N_2O_2S_2$: 488.1592 $[M]^+$; found: 488.1604; elemental analysis calcd (%) for $C_{28}H_{28}N_2O_2S_2$: C 68.82, H 5.78, N 5.73; found: C 68.69, H 5.67, N 5.77.

*(2E,2′E)-3,3′-{5,5′-[10-(2-Ethylhexyl)-10H-phenothiazine-3,7-diyl]bis(thiophene-5,2-diyl)}bis(2-cyanoacrylic acid) (**HL2**)*

Compound **HL2** was synthesized as a black powder in 40% yield according to a similar procedure to that described for **HL1**. $^1$H NMR (400 MHz, [D$_6$]DMSO): $\delta = 8.47$ (s, 2H), 7.99 (d, $J = 4.0$ Hz, 2H), 7.72 (d, $J = 4.0$ Hz, 2H), 7.64–7.61 (m, 4H), 7.19–7.17 (m, 2H), 3.89–3.85 (m, 2H), 1.85–1.81 (m, 1H), 1.46–1.21 (m, 8H), 0.86–0.83 ppm (m, 6H); $^{13}$C NMR (125 MHz, [D$_6$]DMSO): $\delta = 163.6$, 151.8, 146.4, 145.5, 141.4, 133.9, 127.1, 126.0, 124.60, 124.58, 124.5, 117.1, 116.5, 97.8, 50.4, 35.7, 29.7, 27.8, 23.2, 22.4, 13.7, 10.2 ppm; HRMS (MALDI): *m/z* calcd for $C_{36}H_{31}N_3O_4S_3$: 665.1476 $[M]^+$; found: 665.1497; elemental analysis calcd (%) for $C_{36}H_{31}N_3O_4S_3$: C 64.94, H 4.69, N 6.31; found: C 64.72, H 4.65, N 6.18.

*(2E,2′E)-3,3′-{5,5′-[10-(2-Ethylhexyl)-10H-phenothiazine-3,7-diyl]bis(3-hexylthiophene-5,2-diyl)}bis(2-cyanoacrylic acid) (**HL3**)*

Compound **HL3** was synthesized as a red powder in 32% yield according to a similar procedure to that described for **HL1**. $^1$H NMR (400 MHz, [D$_6$]acetone): $\delta = 8.46$ (s, 2H), 7.67 (dd, $J = 8.6$, 2.2 Hz, 2H), 7.63 (d, $J = 2.0$ Hz, 2H), 7.61 (s, 2H), 7.21 (d, $J = 8.4$ Hz, 2H), 4.04–3.94 (m, 2H), 2.91 (t, $J = 7.5$ Hz, 4H), 2.01–1.97 (m, 1H), 1.72 (quint, $J = 7.5$ Hz, 4H), 1.54–1.24 (m, 20H), 0.94–0.83 ppm (m, 12H); $^{13}$C NMR (125 MHz, [D$_6$]acetone): $\delta = 164.5$, 157.6, 152.0, 147.2, 144.6, 129.9, 128.8, 127.0, 126.6, 125.8, 118.1, 117.3, 97.4, 52.1, 37.3, 32.4, 32.0, 31.4, 30.5, 30.3, 29.3, 24.7, 23.8, 23.3, 14.4, 14.3, 11.0 ppm; HRMS (MALDI): *m/z* calcd for $C_{48}H_{55}N_3O_4S_3$: 833.3354 $[M]^+$; found: 833.3377; elemental analysis calcd (%) for $C_{48}H_{55}N_3O_4S_3$: C 69.11, H 6.65, N 5.04; found: C 69.23, H 6.53, N 5.05.

*(2E,2′E)-3,3′-{5′,5′′′-[10-(2-Ethylhexyl)-10H-phenothiazine-3,7-diyl]bis(4-hexyl-[2,2′-bithiophene]-5′,5-diyl)}bis(2-cyanoacrylic acid) (**HL4**)*

Compound **HL4** was synthesized as a black powder in 52% yield according to a similar procedure to that described for **HL1**. $^1$H NMR (400 MHz, [D$_6$]acetone): $\delta = 8.45$ (s, 2H), 7.60–7.57 (m, 4H), 7.55 (d, $J = 2.2$ Hz, 2H), 7.49 (d, $J = 4.0$ Hz, 2H), 7.47 (s, 2H), 7.16 (d, $J = 8.8$ Hz, 2H), 4.01–3.91 (m, 2H), 2.91 (t, $J = 7.8$ Hz, 4H), 2.01–1.98 (m, 1H), 1.72 (quint, $J = 7.6$ Hz, 4H), 1.56–1.26 (m, 20H), 0.94–0.84 ppm (m, 12H); $^{13}$C NMR (125 MHz, [D$_8$]THF): $\delta = 164.5$, 156.4, 146.3, 146.2, 145.9, 143.6, 135.3, 129.9, 129.4, 128.6, 126.9, 126.6, 125.8, 125.2, 124.9, 117.4, 116.9, 98.0, 51.9, 37.3, 32.6, 32.1, 31.6, 29.9, 29.7, 29.6, 24.0, 23.5, 14.4, 10.9 ppm; HRMS (MALDI): *m/z* calcd for $C_{56}H_{59}N_3O_4S_5$: 997.3109 $[M]^+$; found: 997.3133; elemental analysis calcd (%) for $C_{56}H_{59}N_3O_4S_5$: C 67.62, H 6.07, N 4.15; found: C 67.19, H 6.00, N 4.21.

## Acknowledgements

Financial support of this research by the Academia Sinica (AS) and NSC (Taiwan) are gratefully acknowledged. Support from the Instrumental Center of Institute of Chemistry (AS) is also acknowledged.

---

[1] B. O'Regan, M. Grätzel, *Nature* **1991**, *353*, 737–740.

[2] a) A. Mishra, M. K. R. Fischer, P. Bäuerle, *Angew. Chem.* **2009**, *121*, 2510–2536; *Angew. Chem. Int. Ed.* **2009**, *48*, 2474–2499; b) Y.-S. Yen, H.-H. Chou, Y.-C. Chen, C.-Y. Hsu, J. T. Lin, *J. Mater. Chem.* **2012**, *22*, 8734–8747; c) B.-G. Kim, K. Chung, J. Kim, *Chem. Eur. J.* **2013**, *19*, 5220–5230; d) A. Yella, R. Humphry-Baker, B. F. E. Curchod, N. A. Astani, J. Teuscher, L. E. Polander, S. Mathew, J.-E. Moser, I. T. Travernelli, U. Rothlisberger, M. Grätzel, M. K. Nazeeruddin, J. Frey, *Chem. Mater.* **2013**, *25*, 2733–2739.

[3] A. Yella, H.-W. Lee, H. N. Tsao, C. Yi, A. K. Chandiran, M. K. Nazeeruddin, E. W.-G. Diau, C.-Y. Yeh, S. M. Zakeeruddin, M. Grätzel, *Science* **2011**, *334*, 629–634.

[4] a) X. Lu, Q. Feng, T. Lan, G. Zhou, Z.-S. Wang, *Chem. Mater.* **2012**, *24*, 3179–3187; b) X. Ren, S. Jiang, M. Cha, G. Zhou, Z.-S. Wang, *Chem. Mater.* **2012**, *24*, 3493–3499.

[5] a) K. Lim, M. J. Ju, J. Na, H. Choi, M. Y. Song, B. Kim, K. Song, J.-S. Yu, E. Kim, J. Ko, *Chem. Eur. J.* **2013**, *19*, 9442–9446; b) Q. Feng, X. Jia, G. Zou, Z.-S. Wang, *Chem. Commun.* **2013**, *49*, 7445–7447; c) Y. Hua, S. Chang, D. Huang, X. Zhou, X. Zhu, J. Zhao, T. Chen, W.-Y. Wong, W.-K. Wong, *Chem. Mater.* **2013**, *25*, 2146–2153; d) R. Y.-Y. Lin, H. W. Lin, Y.-S. Yen, C.-H. Chang, H.-H. Chou, P.-W. Chen, C.-Y. Hsu, Y.-C. Chen, J. T. Lin, K.-C. Ho, *Energy Environ. Sci.* **2013**, *6*, 2477–2486; e) W. Zeng, Y. Gao, Y. Bai, Y. Wang, Y. Shi, M. Zhang, F. Wan, C. Pan, P. Wang, *Chem. Mater.* **2010**, *22*, 1915–1925; f) M. Zhang, Y. Wang, M. Xu, W. Ma, R. Li, P. Wang, *Energy Environ. Sci.* **2013**, *6*, 2944–2949.

[6] a) G. Li, M. Liang, H. Wang, Z. Sun, L. Wang, Z. Wang, S. Xue, *Chem. Mater.* **2013**, *25*, 1713–1722; b) Y. Wu, X. Zhang, W. Li, Z.-S. Wang, H. Tian, W. Zhu, *Adv. Energy Mater.* **2012**, *2*, 149–156.

[7] a) R. Chen, X. Yang, H. Tian, X. Wang, A. Hagfeldt, L. Sun, *Chem. Mater.* **2007**, *19*, 4007–4015; b) Z.-S. Wang, Y. Cui, Y. Dan-oh, C. Kasada, A. Shinpo, K. Hara, *J. Phys. Chem. C* **2007**, *111*, 7224–7230; c) L. Han, A. Islam, H. Chen, M. Malapaka, B. Chiranjeevi, S. Zhang, X. Yang, M. Yanagida, *Energy Environ. Sci.* **2012**, *5*, 6057–6060.

[8] a) N. Koumura, Z.-S. Wang, S. Mori, M. Miyashita, E. Suzuki, K. Hara, *J. Am. Chem. Soc.* **2006**, *128*, 14256–14257; b) Z.-S. Wang, N. Koumura, Y. Cui, M. Takahashi, H. Sekiguchi, A. Mori, T. Kubo, A. Furube, K. Hara, *Chem. Mater.* **2008**, *20*, 3993–4003; c) H.-C. Ting, C.-H. Tsai, J.-H. Chen, L.-Y. Lin, S.-H. Chou, K.-T. Wong, T.-W. Huang, C.-C. Wu, *Org. Lett.* **2012**, *14*, 6338–6341.

[9] a) D. Cao, J. Peng, Y. Hing, X. Fang, L. Wang, H. Meier, *Org. Lett.* **2011**, *13*, 1610–1613; b) S. J. Kim, D. U. Heo, B. J. Yoo, B. Kim, M. J. Ko, M. J. Cho, D. H. Choi, *Synth. Met.* **2012**, *162*, 2095–2101; c) Q. Li, J. Shi, H. Li, S. Li, C. Zhong, F. Guo, M. Peng, J. Hua, J. Qin, Z. Li, *J. Mater. Chem.* **2012**, *22*, 6689–6696.

[10] a) A. Abbotto, V. Leandri, N. Manfredi, F. De Angelis, M. Pastore, J.-H. Yum, M. K. Nazeeruddin, M. Grätzel, *Eur. J. Org. Chem.* **2011**, 6195–6205; b) A. Abbotto, N. Manfredi, C. Marinzi, F. De Angelis, E. Mosconi, J.-H. Yum, Z. Xianxi, M. K. Nazeeruddin, M. Grätzel, *Energy Environ. Sci.* **2009**, *2*, 1094–1101; c) S. S. Park, Y. S. Won, Y. C. Choi, J. H. Kim, *Energy Fuels* **2009**, *23*, 3732–3736; d) H. Shang, Y. Luo, X. Guo, X. Huang, X. Zhan, K. Jiang, Q. Meng, *Dyes Pigm.* **2010**, *87*, 249–256; e) Y. S. Yang, H. D. Kim, J. H. Ryu, K. K. Kim, S. S. Park, K.-S. Ahn, J. H. Kim, *Synth. Met.* **2011**, *161*, 850–855; f) R. Sirohi, D. H. Kim, S.-C. Yu, S. H. Lee, *Dyes Pigm.* **2012**, *92*, 1132–1137; g) T. Maeda, S. Mineta, H. Fujiwara, H. Nakao, S. Yagi, H. Nakazumi, *J. Mater. Chem. A* **2013**, *1*, 1303–1309; h) Z. Iqbal, W.-Q. Wu, H. Zhang, L. Han, X. Fang, L. Wang, D.-B. Kuang, H. Meier, D. Cao, *Org. Electron.* **2013**, *14*, 2662–2672.

[11] Y.-S. Yen, W.-T. Chen, C.-Y. Hsu, H.-H. Chou, J. T. Lin, M.-C. P. Yeh, *Org. Lett.* **2011**, *13*, 4930–4933.

[12] G. Kim, H. R. Yeom, S. Cho, J. H. Seo, J. Y. Kim, C. Yang, *Macromolecules* **2012**, *45*, 1847–1857.

[13] C.-J. Yang, Y. J. Chang, M. Watanabe, Y.-S. Hon, T. J. Chow, *J. Mater. Chem.* **2012**, *22*, 4040–4049.

[14] a) M. K. Nazeeruddin, P. Péchy, T. Renouard, S. M. Zakeeruddin, R. Humphry-Baker, P. Comte, P. Liska, L. Cevey, E. Costa, V. Shklover, L. Spiccia, G. B. Deacon, C. A. Bignozzi, M. Grätzel, *J. Am. Chem. Soc.* **2001**, *123*, 1613–1624; b) T. Kitamura, M. Ikeda, K. Shigaki, T. Inoue, N. A. Anderson, X. Ai, T. Lian, S. Yanagida, *Chem. Mater.* **2004**, *16*, 1806–1812.

[15] Y.-C. Chen, H.-H. Chou, M. C. Tsai, S.-Y. Chen, J. T. Lin, C.-F. Yao, K. Chen, *Chem. Eur. J.* **2012**, *18*, 5430–5437.

[16] R. Grisorio, L. D. Marco, G. Allegretta, R. Giannuzzi, G. P. Suranna, M. Manca, P. Mastrorilli, G. Gigli, *Dyes Pigm.* **2013**, *98*, 221–231.

[17] S. Agrawal, M. Pastore, G. Marotta, M. A. Reddy, M. Chandrasekharam, F. De Angelis, *J. Phys. Chem. C* **2013**, *117*, 9613–9622.

[18] K. Guo, K. Yan, X. Lu, Y. Qiu, Z. Liu, J. Sun, F. Yan, W. Guo, S. Yang, *Org. Lett.* **2012**, *14*, 2214–2217.

[19] M. K. Nazeeruddin, F. D. Angelis, S. Fantacci, A. Selloni, G. Viscardi, P. Liska, S. Ito, B. Takeru, M. Grätzel, *J. Am. Chem. Soc.* **2005**, *127*, 16835–16847.

[20] a) N. Cai, R. Li, Y. Wang, M. Zhang, P. Wang, *Energy Environ. Sci.* **2013**, *6*, 139–147; b) Z. Ning, Y. Fu, H. Tian, *Energy Environ. Sci.* **2010**, *3*, 1170–1181; c) P. R. Barnes, K. Miettunen, X. Li, A. Y. Anderson, T. Bessho, M. Grätzel, B. C. O'Regan, *Adv. Mater.* **2013**, *25*, 1881–1922.

[21] X. Jiang, K. M. Karlsson, E. Gabrielsson, E. M. J. Johansson, M. Quintana, M. Karlsson, L. Sun, G. Boschloo, A. Hagfeldt, *Adv. Funct. Mater.* **2011**, *21*, 2944–2952.

[22] Q-CHEM, Version 4.0.1, Y. Shao, L. Fusti-Molnar, Y. Jung, J. Kussmann, C. Ochsenfeld, S. T. Brown, A. T. B. Gilbert, L. V. Slipchenko, S. V. Levchenko, D. P. O'Neill, R. A. DiStasio, Jr., R. C. Lochan, T. Wang, G. J. O. Beran, N. A. Besley, J. M. Herbert, C. Y. Lin, T. Van Voorhis, S. H. Chien, A. Sodt, R. P. Steele, V. A. Rassolov, P. E. Maslen, P. P. Korambath, R. D. Adamson, B. Austin, J. Baker, E. F. C. Byrd, H. Dachsel, R. J. Doerksen, A. Dreuw, B. D. Dunietz, A. D. Dutoi, T. R. Furlani, S. R. Gwaltney, A. Heyden, S. Hirata, C.-P. Hsu, G. Kedziora, R. Z. Khaliullin, P. Klunzinger, A. M. Lee, M. S. Lee, W. Liang, I. Lotan, N. Nair, B. Peters, E. I. Proynov, P. A. Pieniazek, Y. M. Rhee, J. Ritchie, E. Rosta, C. D. Sherrill, A. C. Simmonett, J. E. Subotnik, H. L. Woodcock III, W. Zhang, A. T. Bell, A. K. Chakraborty, D. M. Chipman, F. J. Keil, A. Warshel, W. J. Hehre, H. F. Schaefer III, J. Kong, A. I. Krylov, P. M. W. Gill, M. Head-Gordon, Z. Gan, Y. Zhao, N. E. Schultz, D. Truhlar, E. Epifanovsky, M. Oana, R. Baer, B. R. Brooks, D. Casanova, J.-D. Chai, C.-L. Cheng, C. Cramer, D. Crittenden, A. Ghysels, G. Hawkins, E. G. Hohenstein, C. Kelley, W. Kurlancheek, D. Liotard, E. Livshits, P. Manohar, A. Marenich, D. Neuhauser, R. Olson, M. A. Rohrdanz, K. S. Thanthiriwatte, A. J. W. Thom, V. Vanovschi, C. F. Williams, Q. Wu, Z.-Q. You, A. Aspuru-Guzik, C. Chang, R. G. Edgar, E. Sundstrom, J. Parkhill, K. Lawler, M. Gordon, M. Schmit, N. Shenvi, D. Lambrecht, M. Goldey, R. Olivares-Amaya, Y. Bernard, L. Vogt, M. Watson, J. Liu, S. Yeganeh, B. Kaduk, O. Vydrov, X. Xu, I. Kaliman, K. Khistyaev, N. Russ, I. Y. Zhang, W. A. Goddard III, F. Liu, R. King, A. Landau, M. Wormit, A. Dreuw, M. Diedenhofen, A. Klamt, A. W. Lange, D. Ghosh, D. Kosenkov, T. Kus, A. Landou, D. Zuev, J. Deng, S. P. Mao, Y. C. Su, D. Small, L. D. Jacobson, Q-Chem. Inc., Pittsburgh, PA, **2011**.

[23] a) H. M. Vaswani, C.-P. Hsu, M. Head-Gordon, G. R. Fleming, *J. Phys. Chem. B* **2003**, *107*, 7940–7946; b) Y. Kurashige, T. Nakajima, S. Kurashige, K. Hirao, Y. Nishikitani, *J. Phys. Chem. A* **2007**, *111*, 5544–5548.

[24] A. Dreuw, M. Head-Gordon, *J. Am. Chem. Soc.* **2004**, *126*, 4007–4016.

Received: September 9, 2013